An Rb family–independent E2F3 transcription factor variant impairs STAT5 signaling and mammary gland remodeling during pregnancy in mice

Received for publication, October 23, 2017, and in revised form, January 8, 2018 Published, Papers in Press, January 12, 2018, DOI 10.1074/jbc.RA117.000583

Yang Liao and Wei Du[1]

From the Ben May Department for Cancer Research, University of Chicago, Chicago, Illinois 60637

Edited by Xiao-Fan Wang

E2F transcription factors are regulated by binding to the retinoblastoma (Rb) tumor suppressor family of proteins. Previously, we reported an *E2F*^{LQ} mutation that disrupts the binding with Rb proteins without affecting the transcriptional activity of E2F. We also showed that mouse embryonic fibroblasts with an *E2F3*^{LQ} mutation exhibit increased E2F activity and more rapid cell proliferation. In this report, we analyzed *E2F3*^{LQ} mice to further characterize the *in vivo* consequences of Rb family–independent E2F3 activity. We found that homozygous *E2F3*^{LQ} mice were viable and had no obvious developmental defects or tumor growth. Our results also indicated that *E2F3*^{LQ} cells largely retain normal control of cell proliferation *in vivo*. However, female *E2F3*^{LQ} mice had partial nursing defects. Examination of the *E2F3*^{LQ} mammary glands revealed increased caveolin-1 (CAV1) expression, reduced prolactin receptor/Stat5 signaling, and impaired pregnancy-induced cell proliferation and differentiation. Of note, ChIP experiments disclosed that E2F3 binds the CAV1 promoter. Furthermore, E2F3 overexpression induced CAV1 expression, and CRISPR/CAS9-mediated E2F3 knockout reduced CAV1 levels and also increased prolactin receptor–induced Stat5 signaling in mammary epithelial cells. Our results suggest that the Rb family–independent E2F3^{LQ} variant inhibits pregnancy-induced mammary gland cell proliferation and differentiation by up-regulating CAV1 expression and inhibiting Stat5 signaling.

The E2F transcription factors are key cellular targets of the retinoblastoma (Rb)[2] tumor suppressor and are best known for their roles in regulating cell proliferation. In mammalian systems, there are three Rb family proteins (Rb, p107, and p130) and eight E2F family proteins that can be subdivided into three groups: the activating E2Fs (E2F1, 2, and 3), the repressive E2Fs (E2F4 and 5), and the Rb-independent E2Fs (E2F6, 7, and 8) (1–3). Generally speaking, E2F and Rb proteins form complexes during G_1 phase of the cell cycle to repress E2F target gene expression. During G_1/S and S phase, Rb–E2F complexes are disrupted by cyclin-dependent kinase activity, which leads to the release of "free" activating E2F, expression of the E2F target gene, and cell cycle progression. In addition to regulating cell proliferation and DNA replication, *in vivo* studies using animal models revealed that E2F proteins have important roles beyond cell cycle regulation (2–4). Consistent with this, genome-wide studies revealed diverse functions of E2F-regulated genes, including DNA replication and repair, cell cycle regulation, cell cycle checkpoint, cell death, differentiation, etc. (5, 6).

Although the large numbers of E2F targets potentially explain the diverse functions of Rb and E2F proteins, the contribution of the free activating E2F to Rb inactivation–induced developmental and tumor phenotypes remains controversial. On one hand, removing the transcriptional activation function of dE2F1, the only activating E2F in *Drosophila*, can rescue the lethality and gross developmental defects of the fly Rb (*rbf*) mutant (7). Similarly, inactivation of either mouse E2F1 or E2F3 can partially suppress the $Rb^{-/-}$ developmental defects and suppress the $Rb^{+/-}$ mouse pituitary tumor incidence (8–11). Furthermore, the mouse $Rb1^{R654W/+}$ mutation, which corresponds to the human Rb^{R661W} mutation identified in low-penetrance retinoblastomas, reduced the ability to bind activating E2F and promoted pituitary tumor development in a mouse model, similar to the $Rb^{+/-}$ mutation (12–14). These results suggest that inhibition of E2F activity is a critical function of Rb in normal and cancer development in both fly and mammalian systems. On the other hand, loss of either E2F1 or E2F3 in mice can also promote the development of certain cancers, suggesting that the activating E2F proteins also have a tumor suppressor function (9, 11). In addition, the $Rb^{\Delta G}$ mutation, which disrupts the binding between Rb and the E2F transcription activation domain, does not cause spontaneous tumor development despite deregulated E2F target gene expression and accelerated G_1/S transition after serum induction (15). These results could suggest that the free activating E2F proteins are not sufficient to induce tumor development. Alternatively, because the levels of $Rb^{\Delta G}$ appears to be higher than that of the WT Rb, and the Rb family member p107 was shown to be a target of E2F and can bind activating E2F proteins in the absence of Rb (15, 16), it is possible that the altered levels of Rb family proteins contributed to the observed phenotypes. Therefore, despite extensive studies of the Rb and E2F proteins, we still do not

This work was supported by a grant from the University of Chicago Women's Board and NIGMS, National Institutes of Health Grant R01 GM120046 (to W. D.). The authors declare that they have no conflicts of interest with the contents of this article. The content is solely the responsibility of the authors and does not necessarily represent the official views of the National Institutes of Health.

This article contains Figs. S1–S4.

[1] To whom correspondence should be addressed: Ben May Dept. for Cancer Research, University of Chicago, 929 E. 57th St., Chicago, IL 60637. Tel.: 773-834-1949; Fax: 773-702-4476; E-mail: wei@uchicago.edu.

[2] The abbreviations used are: Rb, retinoblastoma; PRL, prolactin; EGF, epidermal growth factor; PRLR, prolactin receptor; MEF, mouse embryonic fibroblast; KO, knockout; FBS, fetal bovine serum; H&E, hematoxylin and eosin; WAP, whey acidic protein; IHC, immunohistochemistry.

know the exact consequences of disrupting the interactions between Rb family proteins and activating E2F *in vivo*.

dE2F1^{su89}, which has an Leu-to-Gln mutation in the conserved Rb binding domain, was originally identified as a suppressor of fly Rb overexpression (17). Importantly, the dE2F1^{su89} mutation disrupts the interaction of dE2F1 with fly Rb without affecting the transcription activation function and can activate E2F target gene expression in the presence of fly Rb proteins (17). Additionally, the LQ mutation in the human C-terminal E2F1 peptide significantly decreased peptide binding to the Rb protein and, more dramatically, to the Rb family protein p107 (18). Furthermore, the same LQ mutation in the full-length mammalian activating E2F proteins also impaired binding of these E2F proteins to the Rb protein without significantly affecting E2F protein levels or the ability to activate transcription (18). Therefore, such Rb family–independent E2F^{LQ} mutations provide useful tools to characterize the roles of the free activating E2F.

Mammary glands mainly consist of the stroma and epithelial cells, which form extensive ductal networks (19, 20). During pregnancy, ductal epithelial cells undergo extensive proliferation and differentiation to form the milk-producing lobuloalveolar units (20, 21). Mammary gland remodeling during pregnancy is regulated by the peptide hormone Prolactin (PRL) in coordination with the steroid hormones and EGF family of growth factors (22, 23). Binding of PRL to the Prolactin receptor (PRLR) induces phosphorylation of signal transducer and activator of transcription 5 (STAT5), which dimerizes and translocates into the nucleus to activate the expression of genes involved mammary epithelium proliferation and differentiation (21). Two STAT5 proteins, STAT5A and STAT5B, have partially redundant functions (24). Interestingly, knockout of Stat5a alone caused lactation defects (25), and inactivation of both Stat5a and Stat5b caused complete absence of lobuloalveolar development, similar to the effect of inactivating PRLR (26). STAT5 activation can also be modulated by several negative regulators, including CAV1, SOCS3, and transforming growth factor β (27–29). CAV1 is the main structural component of caveolae, which are 50- 100-nm invaginations of the plasma membrane involved in signal transduction, transportation, and endocytosis. CAV1 expression is negatively regulated by PRL during lactation (30), and inactivation of CAV1 causes precocious mammary gland development during pregnancy with abnormal activation of STAT5 (27).

In a previous study, we introduced the LQ mutation into mouse E2F3 to generate *E2F3*$^{LQ/LQ}$ knockin mice and characterized the effect of *E2F3*$^{LQ/LQ}$ mutation in mouse embryonic fibroblasts (18). Here we describe the characterization of the effect of Rb family–independent *E2F3*$^{LQ/LQ}$ mutation on mammary gland remodeling during pregnancy.

Results

E2F3$^{LQ/LQ}$ *female mice have a nursing defect*

E2F3$^{LQ/LQ}$ mice can be obtained at the expected ratio and appear indistinguishable from the WT littermates. However, *E2F3*$^{LQ/LQ}$ females have small litter sizes, which is due to the fact that around 60% of the pups do not survive past parturition day 2 (Fig. 1*A*). Although pups from WT mothers have obvious milk spots at parturition day 2, only 40% of pups from *E2F3*$^{LQ/LQ}$ mothers have milk spots (Fig. 1, *B–D*), despite the fact that *E2F3*$^{LQ/LQ}$ mothers exhibit normal maternal care behavior. Additionally, the average weight of pups from *E2F3*$^{LQ/LQ}$ mothers (around 8 g) was significantly less than the average weight of pups from WT mothers (around 10 g) at weaning (Fig. S1). Furthermore, the *E2F3*$^{LQ/LQ}$ mother independently generated from embryonic stem cell clone 172 also showed similar nursing defects. These observations suggest that the *E2F3*$^{LQ/LQ}$ mothers may not have sufficient milk to feed pups. Consistent with this, most (94%) of the pups from *E2F3*$^{LQ/LQ}$ mothers survived when fostered by WT females (Fig. 1*A*). Furthermore, normal weight at weaning was observed for pups from *E2F3*$^{LQ/LQ}$ mothers that were fostered by WT females, whereas a lower weight was observed for pups from WT females that were fostered by *E2F3*$^{LQ/LQ}$ females (Fig. S1). These results suggest that the *E2F3*$^{LQ/LQ}$ females may have defects in producing sufficient milk.

E2F3$^{LQ/LQ}$ *mammary glands exhibit a cell proliferation defect during pregnancy*

We compared the mammary glands from WT and *E2F3*$^{LQ/LQ}$ mice at 8 weeks, during pregnancy, and during lactation. At 8 weeks, female mice reach the mature virgin stage, and the mammary glands develop the general structure of the epithelial tree (Fig. 1*E*). The *E2F3*$^{LQ/LQ}$ mammary glands appeared to have a reduced number of branches compared with those from WT ones at the same stage (Fig. 1, *E* and *F*). This was confirmed by quantification using MammoQuant (31), which revealed a reduced number of internal segments in the *E2F3*$^{LQ/LQ}$ mammary glands (Fig. 1*G*). During pregnancy, mammary epithelial cells will proliferate and form the alveolar structures. The *E2F3*$^{LQ/LQ}$ mammary glands exhibited reduced density of lobuloalveolar structures compared with that observed in the WT ones (Fig. 1, *H–L*). After parturition, lobuloalveolar structures further differentiate into milk-producing alveoli. Again, a higher density of alveoli was observed in WT compared with *E2F3*$^{LQ/LQ}$ mammary glands (Fig. 1, *M–O*). Therefore the *E2F3*$^{LQ/LQ}$ mammary glands have reduced milk-producing alveoli, which may contribute to the observed nursing defect.

Because mammary glands undergo massive cell proliferation during pregnancy, we further characterized whether the reduction in alveolar structures in *E2F3*$^{LQ/LQ}$ mammary glands is due to changes in cell proliferation and differentiation. A significantly reduced level of the cell proliferation marker Ki67 was observed in *E2F3*$^{LQ/LQ}$ compared with that of the WT mammary glands (Fig. 2, *A–C*). These results suggest that *E2F3*$^{LQ/LQ}$ mammary glands have reduced cell proliferation, which leads to reduced milk-producing alveolar structures. Interestingly, although *E2F3*^{LQ} mutation is expected to increase E2F target gene expression, slightly reduced E2F target gene expression was observed in these mammary glands (Fig. S2A). These observations are likely due to the combined effects of reduced level of S/G_2/M cells and higher E2F target gene expression in G_1 cells in the *E2F3*^{LQ} mammary glands. Indeed, expression of E2F target genes such as *Ccne1*, *Ccna2*, and *PCNA* was elevated in quiescent 15-week-old virgin *E2F3*$^{LQ/LQ}$ mammary glands in comparison with the WT controls (Fig. S2, *B* and *C*). Taken together, these

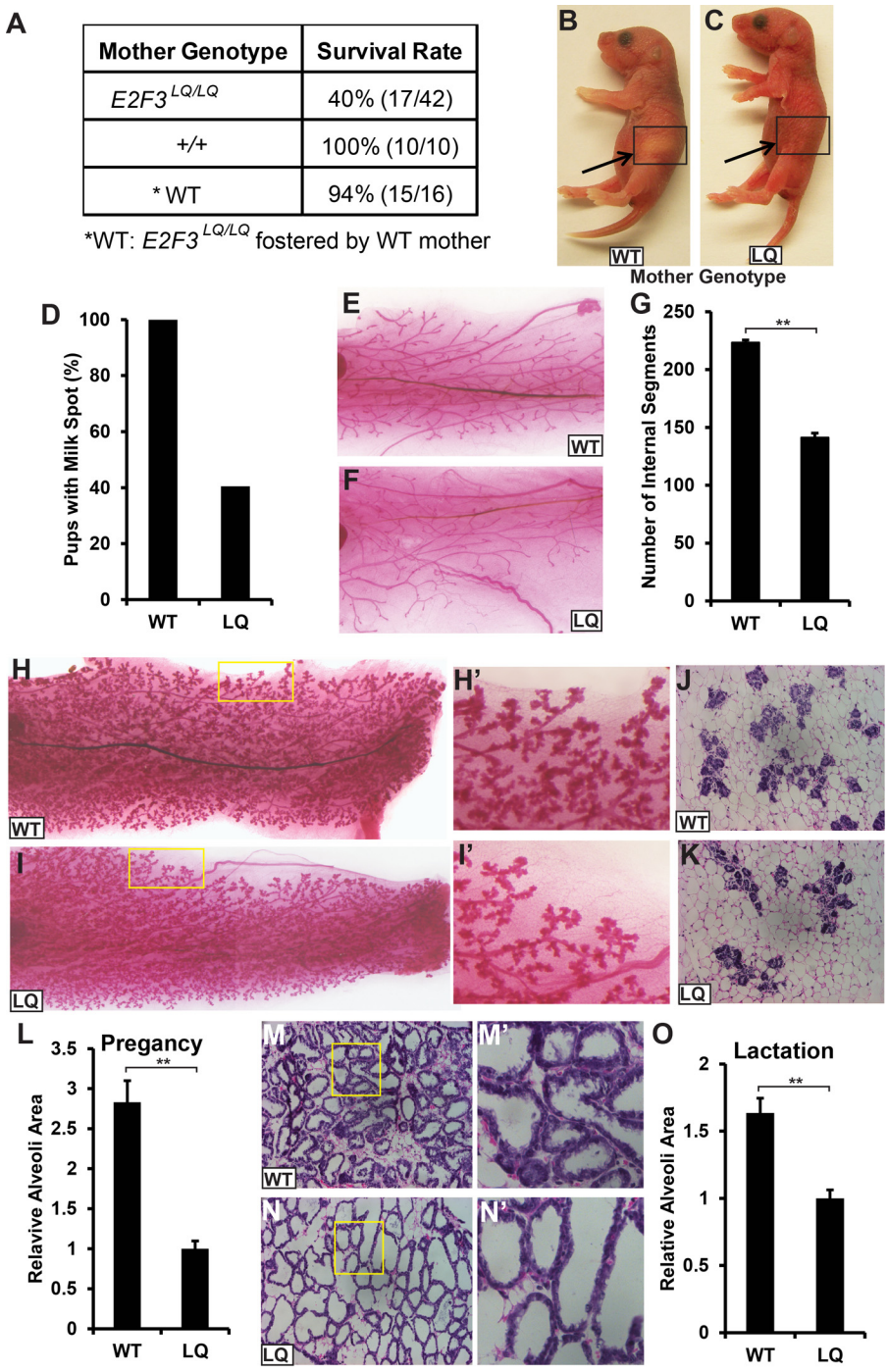

Figure 1. E2F3$^{LQ/LQ}$ mice show nursing and mammary gland defects. *A*, the survival rate of pups from each genotype mother 2 days after parturition. *B* and *C*, pictures of a pup from a WT mother with a white milk spot in the stomach (*B*) and a pup from an E2F3$^{LQ/LQ}$ mother without an obvious milk spot in its stomach (*C*). *D*, quantification of pups with milk spots from a WT ($n = 10$ pups) or LQ mother ($n = 42$ pups) 2 days after parturition. *E* and *F*, whole-mount staining of an 8-week mammary gland from WT (*E*) and *E2F3*$^{LQ/LQ}$ (*F*) mice. *G*, quantification of internal segments of WT ($n = 6$) and LQ ($n = 6$) glands at 8 weeks by MammoQuant. *H* and *I*, whole-mount staining of mammary glands of WT (*H*) and *E2F3*$^{LQ/LQ}$ (*I*) pregnant mice. The rectangles in (*H*) and (*I*) are showing regions that are enlarged in *H′* and *I′*. *J* and *K*, H&E staining of pregnant mammary glands of WT (*J*) and LQ (*K*) mice. *L*, quantification of the relative alveolar area of WT ($n = 6$) and LQ ($n = 6$) glands from pregnancy day 15 females. *M* and *N*, H&E staining of day 3 lactating mammary glands of WT (*M*) and LQ (*N*) mice. The squares in (*M*) and (*N*) are showing regions that are enlarged in *M′* and *N′*. *O*, quantification of the relative alveolar area of WT ($n = 6$) and LQ ($n = 6$) glands at lactation. All graphs represent the mean ± S.D. **, $p < 0.01$.

results suggest that the reduced cell proliferation in *E2F3*$^{LQ/LQ}$ mammary glands is likely due to the effect of the *E2F3*^{LQ} mutation on certain signaling pathways regulating mammary gland proliferation instead of its direct effect on the expression of cell cycle regulators. In addition, these data also show that the presence of free E2F3 does not prevent cells from staying in the quiescent state.

E2F3$^{LQ/LQ}$ *mammary glands also exhibit cell differentiation defects*

We further tested the effect of *E2F3*^{LQ} mutation on the expression of mammary gland differentiation genes. Expression of the milk genes *Wap* and *Csn2*, which are expressed in the differentiated alveolar cells, was dramatically decreased in

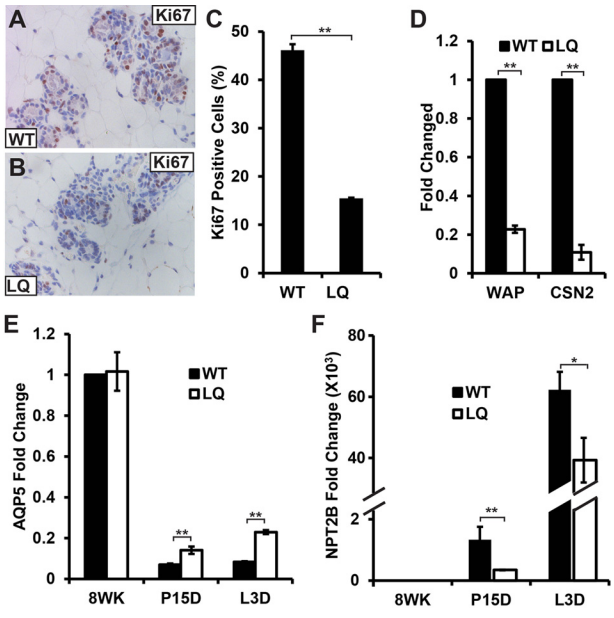

Figure 2. E2F3$^{LQ/LQ}$ mammary glands showed defects in proliferation and differentiation. *A* and *B*, cell proliferation assessed by Ki67 IHC staining in WT (*A*) and E2F3$^{LQ/LQ}$ (*LQ*, *B*) glands at pregnancy. *C*, quantification of Ki67-positive cells in WT ($n = 6$) and LQ ($n = 6$) glands at pregnancy. *D*, quantitative real-time PCR analysis of the milk genes *Wap* and *Csn2* in WT and LQ glands at lactation. *E* and *F*, quantitative real-time PCR analysis of the mammary gland differentiation markers *Aqp5* (*E*) and *Npt2b* (*F*) in WT and LQ glands at 8 weeks (*8WK*), pregnancy (*P15D*), and lactation (*L3D*). All graphs represent mean ± S.D. *, $p < 0.05$; **, $p < 0.01$.

lactating *E2F3*$^{LQ/LQ}$ mammary glands (Fig. 2*D*). The reduction in milk gene expression appeared to be more dramatic than the moderate reduction in the amount of alveolar structures, suggesting that *E2F3*$^{LQ/LQ}$ mammary glands may have an additional defect in differentiation.

We further characterized two additional differentiation markers, Aquaporin (Aqp5) and sodium P_i cotransporter isoform (Npt2b), at different mammary gland development stages. Aqp5, which is expressed in the virgin mammary glands, is repressed as mammary ductal epithelium differentiates into alveolar cells (32). Although the expression of Aqp5 was repressed in both WT and *E2F3*$^{LQ/LQ}$ mammary glands during pregnancy and lactation, significantly higher levels of Aqp5 expression were detected in *E2F3*$^{LQ/LQ}$ mammary glands (Fig. 2*E*). In contrast, Npt2b, which is not expressed in virgin mammary glands, is strongly expressed in differentiated alveolar cells (26, 32). Significantly reduced Npt2b expression was observed in *E2F3*$^{LQ/LQ}$ mammary glands during the pregnancy and lactation stage (Fig. 2*F*). Taken together, these results show that the *E2F3*$^{LQ/LQ}$ mammary glands also have defects in alveolar differentiation.

E2F3$^{LQ/LQ}$ *mutation decreases PRLR/STAT5 signaling during mammary gland development*

Activation of PRLR in the mammary gland leads to the phosphorylation and nuclear translocation of STAT5, which induces the expression of PRLR/STAT5 signaling targets, including RankL and Cyclin D1 (21, 25). Because the *E2F3*$^{LQ/LQ}$ mammary gland phenotypes have similarity to the previously described phenotypes of PRLR-deficient, Stat5a conditional knockout, or RANKL knockout mice (25, 33, 34), we hypothesize that *E2F3*$^{LQ/LQ}$ may negatively regulate PRLR/STAT5 signaling during mammary gland development.

We first used STAT5 and p-STAT5 antibody to characterize the effect of *E2F3*$^{LQ/LQ}$ mutation on PRLR/STAT5 signaling. STAT5 signaling is activated in the 8-week-old virgin mammary glands, as shown by the accumulation of phosphorylated STAT5 (pSTAT5) in the nucleus of luminal cells (Fig. 3*A*). Although *E2F3*$^{LQ/LQ}$ mutation did not decrease the level of STAT5 protein (Fig. 3, *B* and *D*), the number of cells with high levels of p-STAT5 were significantly reduced in the *E2F3*$^{LQ/LQ}$ mammary glands (Fig. 3, *A* and *C*). Additionally, a significantly decreased number of high p-STAT5 expressing cells were also observed in the *E2F3*$^{LQ/LQ}$ mammary glands during pregnancy (Fig. 3, *E–I*) as well as lactation (Fig. 3, *J–L*). The decreased p-STAT5 but not total STAT5 levels in different-stage *E2F3*$^{LQ/LQ}$ mammary glands were also confirmed by Western blots (Fig. 3M). Furthermore, functionally important target genes of PRLR/STAT5 signaling, such as *RankL*, *Ccnd1*, *Gjb2*, *Csn2*, and *Wap* (21), were also significantly decreased in *E2F3*$^{LQ/LQ}$ mammary glands during both pregnancy and lactation stages (Figs. 2*D* and 3*N*). Collectively, *E2F3*$^{LQ/LQ}$ mutation results in decreased PRLR/STAT5 signaling and expression of the PRLR/STAT5 target genes.

E2F3 regulates CAV1 expression

To determine how *E2F3*$^{LQ/LQ}$ mutation affects PRLR/STAT5 signaling, we tested the expression of regulators and components of PRLR/STAT5 signaling in the pregnant stage WT or *E2F3*$^{LQ/LQ}$ mammary glands by quantitative real-time PCR. CAV1, a negative regulator of PRLR/STAT5 signaling, was significantly increased in *E2F3*$^{LQ/LQ}$ mammary glands (Fig. 4*A*). In addition, PRLR and Elf5, which promote STAT5 signaling, were found to be decreased (Fig. 4*A*).

Previous studies showed that CAV1 plays important roles in mammary gland development. *CAV1*$^{-/-}$ mice displayed accelerated development of the lobuloalveolar compartment in the mammary glands (27). CAV1 was shown to bind to JAK2, decrease STAT5 phosphorylation, and reduce PRLR/STAT5 signaling (27). To determine whether the CAV1 protein level was also increased in *E2F3*$^{LQ/LQ}$ glands, we stained lactation-stage mammary gland samples with CAV1 antibody. *E2F3*$^{LQ/LQ}$ glands showed a significantly higher level of CAV1 than wild-type glands (Fig. 4, *B* and *C*). Furthermore, we compared the CAV1 levels in WT and *E2F3*$^{LQ/LQ}$ mammary glands from different developmental stages by Western blots. As shown in previous studies (30), CAV1 protein was highest in virgin-stage glands and decreased in pregnancy- and lactation-stage glands (Fig. 4*D*). Importantly, *E2F3*$^{LQ/LQ}$ mammary glands showed a significantly higher level of CAV1 than the WT glands in all three stages (Fig. 4*D*). We also compared the CAV1 protein levels in different tissues from WT and *E2F3*$^{LQ/LQ}$ mice. *E2F3*$^{LQ/LQ}$ mutation significantly increased CAV1 levels in mammary glands but not in other tissues examined (Fig. 4*E*). Therefore the regulation of CAV1 by E2F3 appears to be tissue-specific. Interestingly, the levels of E2F1 and E2F2 were reduced in E2F3^{LQ} mammary glands but not in other tissues (Fig. S3). It is possible that the decreased levels of

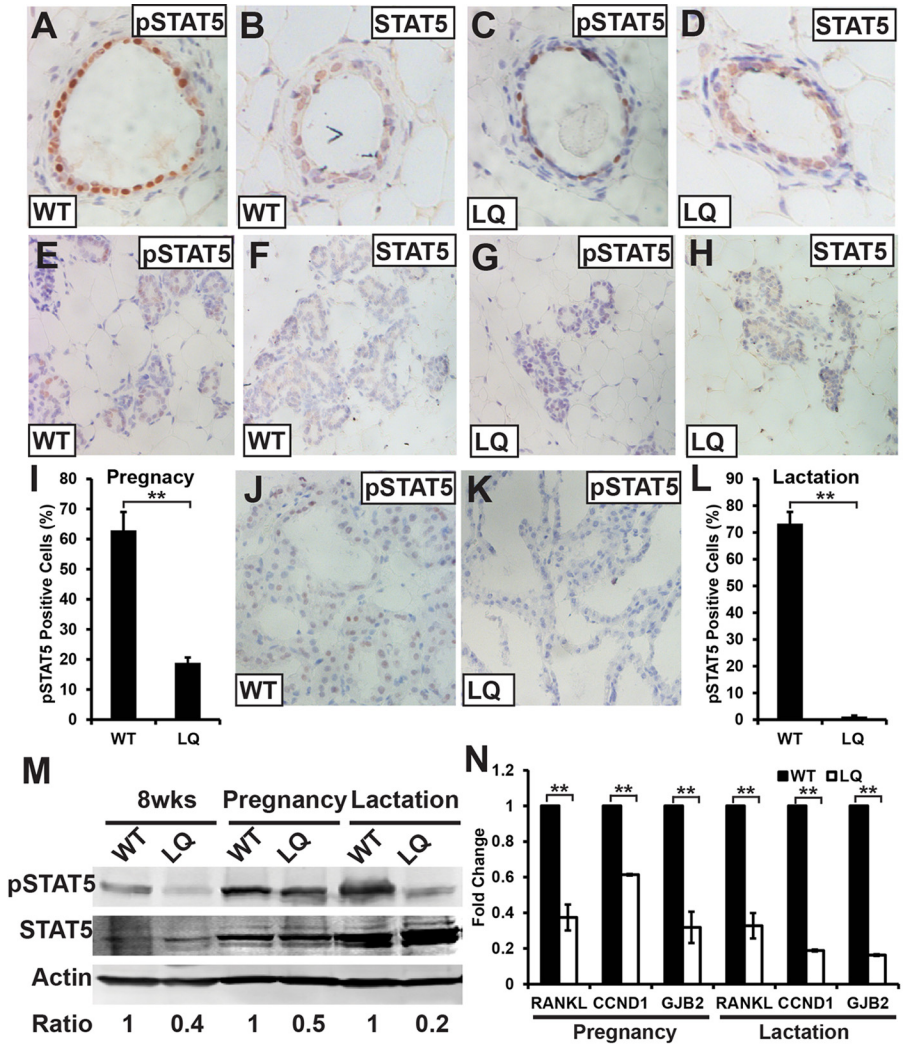

Figure 3. E2F3$^{LQ/LQ}$ mammary glands showed reduced STAT5 signaling. *A–D*, IHC staining for pStat5 and Stat5 in WT (*A* and *B*) and *E2F3*$^{LQ/LQ}$ (*LQ*) (*C* and *D*) glands at 8 weeks. *E–H*, IHC staining of pStat5 and Stat5 in WT (*E* and *F*) and LQ (*G* and *H*) glands at pregnancy. *I*, quantification of pSTAT5-positive cells in WT ($n = 6$) and LQ ($n = 6$) glands at pregnancy. *J* and *K*, IHC staining for pStat5 in WT (*J*) and LQ (*K*) glands at lactation. *L*, quantification of pSTAT5-positive cells in WT ($n = 6$) and LQ ($n = 6$) glands at lactation. *M*, immunoblot assay of pSTAT5 and STAT5 proteins in lysates prepared from WT and LQ glands at 8 weeks and pregnancy and lactation stages. β-Actin was used as a loading control. The ratio showed the relative band intensity of pSTAT5 in WT and LQ samples, which were normalized with the band intensity of STAT5. The band intensity was measured from three independent experiments by Image Studio (ver. 2.1). *N*, quantitative real-time PCR analysis of the STAT5 signaling target genes Rankl, Ccnd1, and Gjb2 in WT and LQ glands at pregnancy and lactation. All graphs represent mean ± S.D. **, $p < 0.01$.

E2F1/2 in complex with the Rb protein in mammary glands may contribute to the observed effects of E2F3^{LQ} mutation on CAV1 expression.

Although CAV1 has not been shown to be regulated by E2F, an E2F binding site was observed in the CAV1 promoter region (35) (Fig. 5*A*). To determine whether E2F3 binds to the E2F site in the CAV1 promoter *in vivo*, we carried out a ChIP experiment using MCF10A non-transformed mammary epithelial cells. Indeed, the ChIP experiment revealed that endogenous E2F3 bound to the E2F site region in the CAV1 promoter but not to the upstream control region 9 kb away (Fig. 5, *A* and *B*). To further determine the effect of the E2F3^{LQ} mutation on the binding of Rb to this region, we carried out Rb ChIP in WT and E2F3^{LQ} MEFs. As shown in Fig. S4, Rb also bound specifically to the CAV1 promoter region, and the binding was reduced in the presence of the E2F3^{LQ} mutation (Fig. S4).

To determine whether E2F3 regulates CAV1 expression, we first examined the effect of E2F3 overexpression. Overexpression of E2F3 led to increased CAV1 levels in both MCF10A and HC11 mammary epithelial cells (36) (Fig. 5, *C* and *D*). Therefore, E2F3 binds to the CAV1 promoter and is sufficient to induce CAV1 expression in mammary epithelial cells.

To further characterize whether E2F3 is required for CAV1 expression in mammary epithelial cells, we used the CRISPR/Cas9 system (37) to knock out E2F3 in HC11 mammary epithelial cells. Two independent E2F3 KO clones were established and verified by sequencing (Fig. 5*E*). Interestingly, KO of E2F3 significantly down-regulated CAV1 levels (Fig. 5*F*). Therefore, E2F3 is also required for the expression of CAV1 in mammary epithelial cells. Taken together, these results suggest that E2F3 directly regulates CAV1 expression.

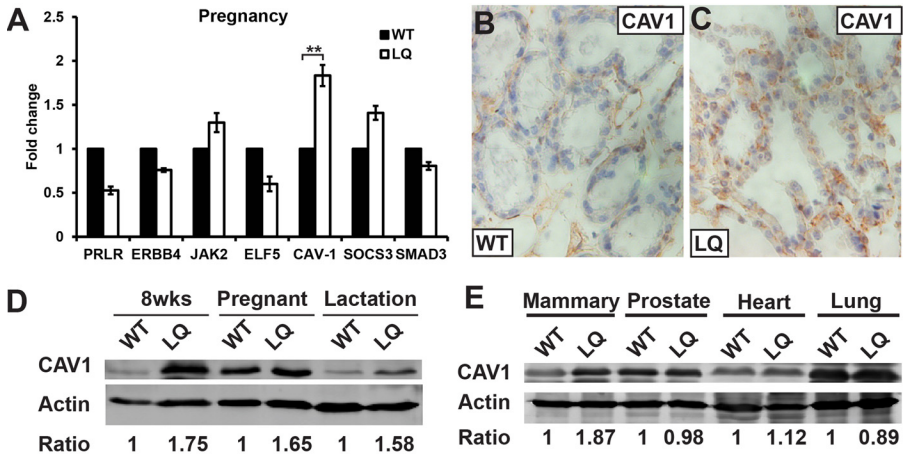

Figure 4. CAV1 expression was elevated in *E2F3*$^{LQ/LQ}$ mammalian glands. *A*, quantitative real-time PCR analysis of the STAT5 signaling-related genes PRLR, Erbb4, Jak2, Elf5, CAV1, Socs3, and Smad3 in WT and *E2F3*$^{LQ/LQ}$ (*LQ*) glands at pregnancy. *B* and *C*, IHC staining for CAV1 in WT (*B*) and LQ (*C*) glands at lactation. *D*, immunoblot assay of CAV1 proteins in the lysates prepared from WT and LQ glands at 8 weeks, pregnancy, and lactation. β-Actin was used as a loading control. The ratio shows the relative band intensity of CAV1 in samples, which were normalized with the band intensity of actin. The band intensity was measured from three independent experiments by Image Studio (ver. 2.1). *E*, immunoblot assay of CAV1 proteins in the lysates prepared from WT and LQ tissue samples. β-Actin was used as a loading control. The ratio was calculated as in *D*.

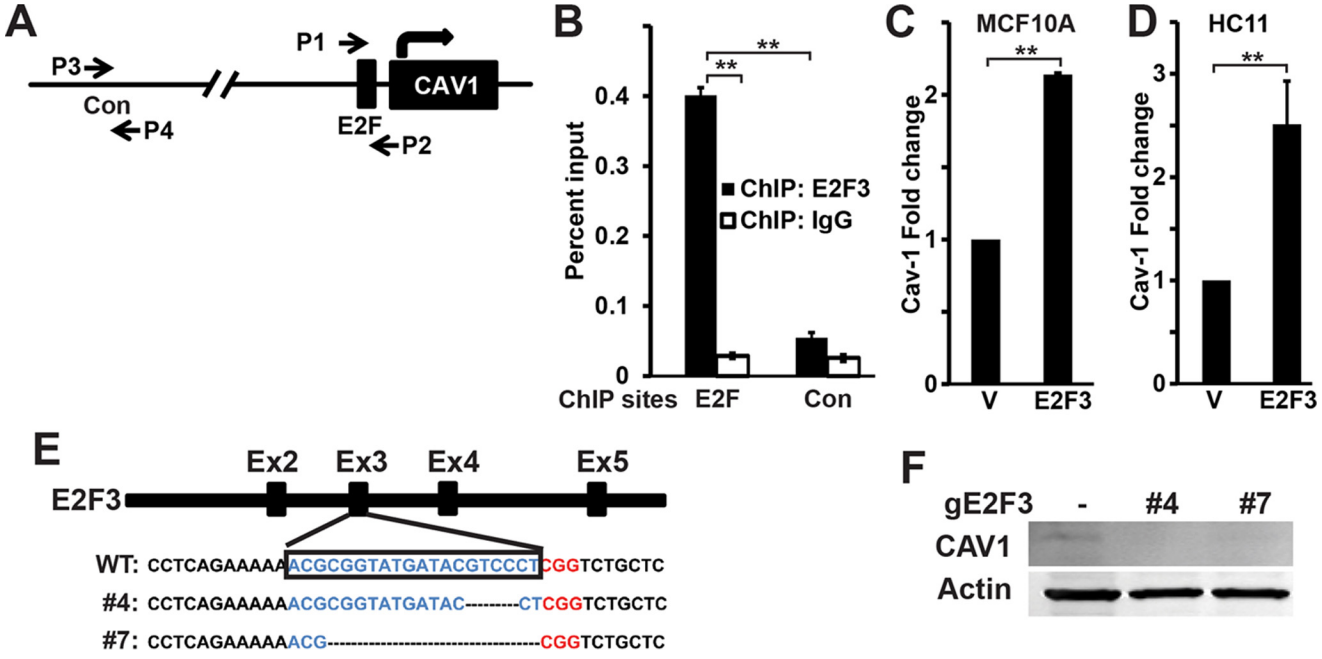

Figure 5. E2F3 bound to the CAV1 promoter and induced CAV1 expression in mammary epithelial cells. *A*, schematic showing the human CAV1 promoter. Primers (*P1* and *P2*) were used to amplify the region that contains a putative E2F binding site (*E2F*). Primers (*P3* and *P4*) were used to amplify the control region that is up 9 kb of the putative E2F binding site (*Con*). *B*, ChIP analysis for the binding of E2F3 to the consensus site in the CAV1 promoter in MCF10A cells with E2F3 antibody. IgG antibody served as a negative control. MCF10A cells were treated with 0.75% formaldehyde for 10 min and processed for ChIP analysis. The occupancy of E2F3 of the CAV1 promoter was detected by real-time PCR as indicated in *A*. Three independent ChIP experiments were carried out with similar results. The data from one representative ChIP experiment are shown. *C* and *D*, quantitative real-time PCR analysis was carried out to determine the effect of E2F3 overexpression on CAV1 expression in MCF10A (*C*) and HC11 (*D*) cells. *V*, control cells. *E*, sequence analysis of CRISPR/Cas9-induced targeted deletion mutations in the E2F3 coding region in HC11 cell clones 4 and 7. Single guide RNA sequences are shown in *blue*, and the protospacer adjacent motif sequence is shown in *red*. The deleted sequence is shown as a *dashed line*. *F*, immunoblot assay of CAV1 protein in lysates prepared from HC11 wildtype and E2F3 knockout clones 4 and 7. β-Actin was used as a loading control. All graphs represent mean ± S.D. **, $p < 0.01$.

CAV1 contributes to the effect of E2F3 on PRLR/STAT5 signaling and lactogenesis

We used the well-established HC11 lactation model (36) to further characterize the contribution of CAV1 on the regulation of PRLR/STAT5 signaling and lactogenesis by E2F3. Similar to the *in vivo* situation, prolactin-induced lactogenic differentiation in HC11 cells is associated with STAT5 activation, as shown by increased p-STAT5 levels (Fig. 6*A*). Interestingly, both E2F3 knockout clones significantly increased PRLR-induced p-STAT5 levels (Fig. 6*A*) and milk gene expression (Fig. 6*B*). In contrast, E2F3 overexpression in HC11 cells significantly decreased prolactin-induced p-STAT5 levels (Fig. 6*D*, *lanes 7* and *8*) and decreased lactogenic differentiation, as shown by reduced milk gene expression (Fig. 6*E*, *lanes 1* and *2*). These data show that E2F3 negatively regulates PRLR/STAT5 signaling and lactogenesis.

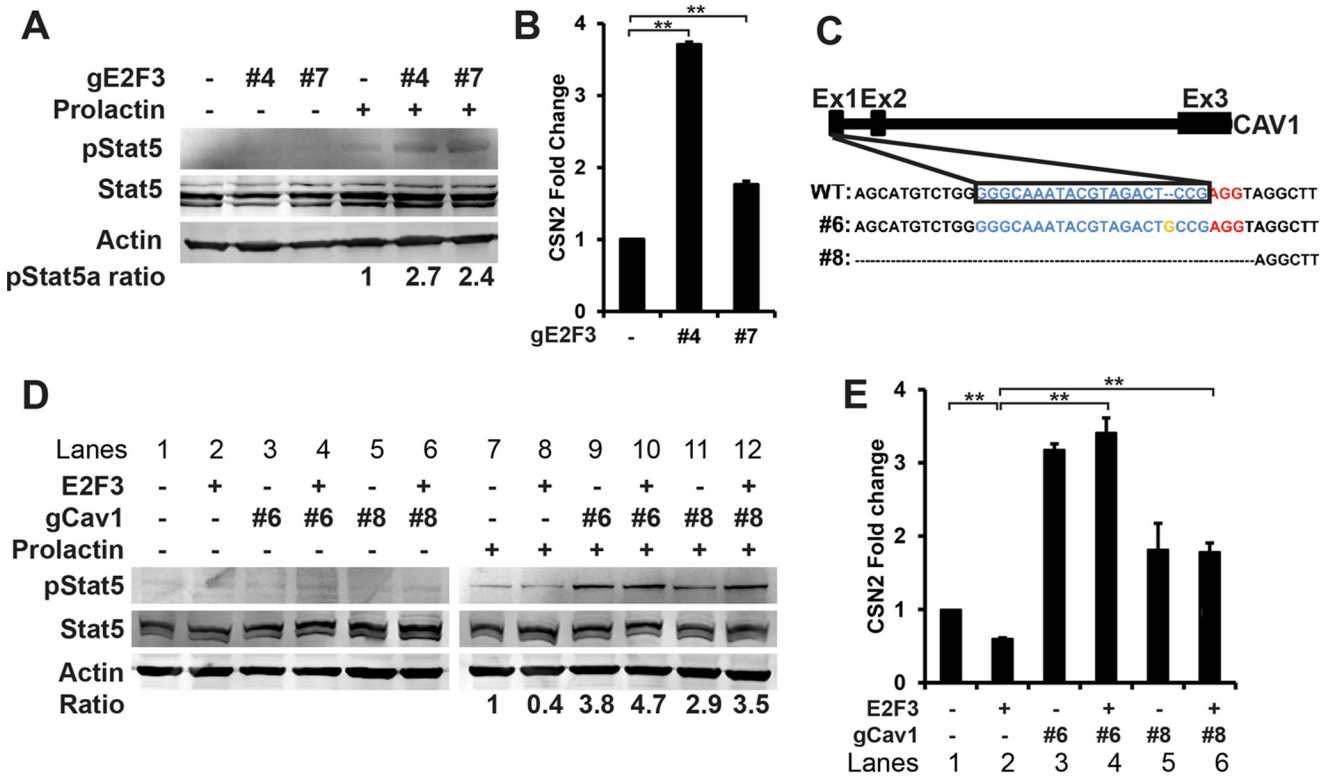

Figure 6. E2F3 modulated STAT5 signaling through CAV1. *A*, immunoblot assay of pSTAT5 and STAT5 proteins in lysates prepared from wildtype and E2F3 knockout clone 4 and 7 cells with or without the induction of prolactin. β-Actin was used as a loading control. The ratio shows the relative band intensity of pSTAT5 in samples, which were normalized with the band intensity of STAT5. The band intensity was measured from three independent experiments by Image Studio (ver. 2.1). *B*, quantitative real-time PCR analysis of the milk gene Csn2 in wildtype and E2F3 knockout clones 4 and 7 with the induction of prolactin. *C*, sequence analysis of CRISPR/Cas9-induced indel mutations in targeted regions of CAV1 in HC11 cell clones 6 and 8. Single guide RNA sequences are shown in *blue*, and the protospacer adjacent motif sequence is shown in *red*. The inserted sequence is shown in *orange*. The deleted sequence is shown as a *dashed line*. *D*, immunoblot assay of pSTAT5 and STAT5 proteins in the lysates prepared from wildtype and CAV1 knockout clone 6 and 8 cells under the indicated conditions. β-Actin was used as a loading control. The ratio was calculated as described in *A*. *E*, quantitative real-time PCR analysis of the milk gene Csn2 in wildtype and CAV1 knockout clones 6 and 8 under the indicated conditions. All graphs represent mean ± S.D. **, $p < 0.01$.

Because E2F3 regulates CAV1 expression in mammary glands, we used the CRISPR/Cas9 approach and generated two independent CAV1 KO clones from HC11 cells. Both clones were verified by sequencing (Fig. 6*C*). Consistent with the idea that CAV1 negatively regulates PRLR/STAT5 signaling and lactogenic differentiation, CAV1 knockout led to significantly higher prolactin-induced p-STAT5 levels (Fig. 6*D*, *lanes 7*, *9*, and *11*) and milk gene expression (Fig. 6*E*, *lanes 1*, *3*, and *5*). Furthermore, E2F3 overexpression in CAV1 KO HC11 cells did not decrease p-STAT5 levels (Fig. 6*D*, compare *lanes 9* and *10*, *11*, and *12*) or milk gene expression (Fig. 6*E*). These results strongly support the idea that CAV1 contributes to the effect of $E2F3^{LQ}$ mutation on PRLR/STAT5 signaling and lactogenesis in mammary epithelial cells (Fig. 7).

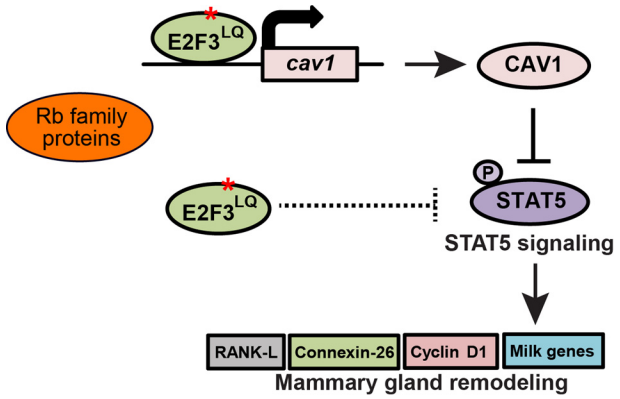

Figure 7. A model showing E2F3, STAT5 signaling, and mammary gland remodeling. $E2F3^{LQ}$ mutation causes elevated CAV1 expression, which inhibits STAT5 activation and impairs pregnancy-induced mammary gland remodeling. In addition, $E2F3^{LQ}$ mutation may inhibit STAT5 signaling through additional mechanisms, such as decreasing the level of PRLR.

Discussion

In this report, we show that the nursing defect of the $E2F3^{LQ/LQ}$ females is correlated with defective PRLR/STAT5 signaling, reduced cell proliferation, and impaired differentiation in mammary glands during pregnancy. We demonstrate that CAV1 is a direct target of E2F3 in mammary glands and that $E2F3^{LQ/LQ}$ mammary glands show increased CAV1 expression, which contributes to decreased PRLR signaling and reduced pregnancy-induced mammary gland proliferation and differentiation. Therefore, disrupting the Rb family and E2F interaction may regulate cell proliferation indirectly through modulating tissue-specific signaling pathways in addition to the well-established effects on the cell cycle. Interestingly, CAV1 has been suggested to be a suppressor of mammary tumor growth and metastasis. CAV1 knockout was shown to significantly promote mammary tumor growth and metastasis (38–40). Additionally, high stromal CAV1 levels are associated with reduced breast cancer metastasis and improved survival

(41). Therefore, it will be interesting to test whether the increased expression of CAV1 in E2F3$^{LQ/LQ}$ will affect breast cancer development.

CAV1 is known to play a role in mammary gland development through modulating the activation of STAT5A (27). A study showed that prolactin induces the transcriptional down-regulation of CAV1 expression during pregnancy and suggested that the down-regulation might be dependent on Ras-p42/44 mitogen-activated protein kinase (30). However, the detailed mechanism of the regulation of CAV1 is largely unknown. In this study, we show that CAV1 is a novel target gene of E2F3. Interestingly, CAV1 is only found to be up-regulated in the mammary glands of *E2F3*$^{LQ/LQ}$ mice. Although the exact regulatory mechanisms of CAV1 by E2F3 require further investigation, the tissue-specific regulation of CAV1 by E2F3 could be the reason why CAV1 was not identified as a direct E2F transcriptional target.

Inactivation of Rb using WAP-Cre in the p107 mutant background resulted in mutant mice that also exhibited lactation defects (42). The exact cause of the lactation defects was not characterized, and it is not clear whether increased CAV1 and reduced Stat5 signaling are also involved in these mice (42). On the other hand, the *E2F3*$^{LQ/LQ}$ mammary gland phenotypes are distinct from those from the *Rb*$^{\Delta L}$ and *Rb*^{NF} mice, which carry mutations that disrupt the interactions between Rb and LXCXE motif–containing proteins (43). The nursing defects of the *Rb*$^{\Delta L}$ and *Rb*^{NF} mice were shown to be associated with increased hyperplastic ducts and defective growth inhibition by transforming growth factor β (43). Interestingly, although some level of hyperplastic ducts were observed in *Rb*$^{\Delta G/\Delta G}$ mice, which contain mutations that disrupt the interactions between Rb and the E2F C-terminal domain, the *Rb*$^{\Delta G/\Delta G}$ mice did not exhibit nursing defects (15). Because *Rb*$^{\Delta G/\Delta G}$ mutation disrupts its interactions with E2F1, E2F2, as well as E2F3, one might have expected that mammary glands from *Rb*$^{\Delta G/\Delta G}$ would show more severe phenotypes than those from *E2F3*$^{LQ/LQ}$. However, because both Rb and p107 are targets of E2F that are up-regulated in the absence of Rb and E2F binding (5, 44), it is possible that the increased level of Rb family proteins, which can bind WT E2F3 but not the *E2F3*$^{LQ/LQ}$ mutant, may partially compensate for the loss of Rb and E2F interaction in *Rb*$^{\Delta G/\Delta G}$ but not *E2F3*$^{LQ/LQ}$ mammary glands. Consistent with this, both p107 and p130 was shown to bind to activating E2F proteins in the absence of pRb (16). In addition, in contrast to the *Rb*$^{\Delta G/\Delta G}$ and *Rb*$^{\Delta L/\Delta L}$ mice, no significantly hyperplastic ducts were observed in *E2F3*$^{LQ/LQ}$ mammary glands. Instead we observed significantly reduced STAT5 signaling and milk gene expression. These results suggest that the hyperplastic duct phenotypes depend on the disruption of all of the Rb–E2F complexes, whereas the regulation of STAT5 signaling and CAV1 expression depend more on the presence of free E2F3.

The deregulated E2F target gene expression and early onset of S phase in response to serum induction observed in *E2F3*$^{LQ/LQ}$ MEFs were similar to those from the *Rb*$^{-/-}$ as well as the *Rb*$^{\Delta G/\Delta G}$ mutant (15, 18, 45). These observations are consistent with a previous study of *E2F3*$^{-/-}$ MEFs, which showed that E2F3 plays critical roles regulating E2F target gene expression and cell proliferation in MEFs (46). However, despite significant deregulated E2F target gene expression, the *E2F3*$^{LQ/LQ}$ and *Rb*$^{\Delta G/\Delta G}$ mice as well as the *dE2F1*^{su89} flies develop normally with little obvious developmental defects (15, 17). The partial lethality and muscle differentiation defects observed in the *Rb*$^{\Delta G/\Delta G}$ mice appears to depend on the genetic background (15). In addition, neither the *E2F3*$^{LQ/LQ}$ nor the *Rb*$^{\Delta G/\Delta G}$ mice exhibit increased tumor development. Therefore, cells with disruption of the Rb and E2F interaction retains normal growth and proliferation regulation *in vivo* and is unable to induce tumor development in the WT background despite showing increased cell growth and proliferation under *in vitro* cell culture conditions in the presence of excess growth factors and nutrients. It appears that disrupting the interactions between endogenous E2F3 and the Rb family affect the rate of cell proliferation instead of the control of a cell to proliferate or stay quiescent, in addition to affecting specific signaling pathways that may regulate cell proliferation and differentiation.

E2F3 was found to be amplified or overexpressed in some cancers (47), and high nuclear E2F3 levels are correlated with poor survival (48). However, as E2F3 overexpression may lead to the deregulation of many more genes than normal E2F targets, it is not clear whether *E2F3*^{LQ}-type mutations that lead to the presence of free E2F3 will affect cancer development. Interestingly, although cancer genome sequencing did not find E2F1, E2F2, or E2F3 to be significantly mutated in cancers (49), several E2F mutations in the Rb binding domain can be found in the Catalogue of Somatic Mutations in Cancer (COSMIC) from the Wellcome Trust Sanger Institute (50). Because the Rb binding domain of E2F overlaps with the transactivation domain, it is possible that mutations that disrupt Rb family binding but retain the transactivation function are quite rare. Further studies of the effect of *E2F3*^{LQ} on cancer development using specific tumor models will shed lights on the effect of disrupting the Rb and E2F interaction on tumor development.

Experimental procedures

Mouse experiment

All animals were housed and treated in accordance with protocols approved by the Institutional Animal Care and Use Committee at the University of Chicago.

Cell culture

HC11 cells (kindly provided by Dr. Zhe Li, Harvard Medical School) were maintained in RPMI medium supplemented with 10% FBS, 50 units/ml Penicillin/Streptomycin, 10 ng/ml EGF, and 5 μg/ml insulin. To analyze cell differentiation, HC11 cells were grown to confluency. After 2 days, the medium of the confluent dishes was changed to RPMI supplemented with 10% FBS, 50 units/ml P/S, 5 μg/ml insulin, and 100 nM dexamethasone (Sigma) with or without 5 μg/ml prolactin (Sigma). For pStat5 detection, HC11 cells were serum-starved in HC11 growth medium without FBS and EGF for 16–20 h and then induced with prolactin (36, 51). MCF10A cells were cultured in Dulbecco's modified Eagle's medium/F12 medium supplemented with 5% horse serum, 20 ng/ml EGF, 10 μg/ml insulin, 0.5 mg/ml hydrocortisone, 1 mg/ml cholera toxin, 50 international units penicillin/streptomycin, and 2 mmol/liter L-glutamine. MEF cells were cultured in Dulbecco's modified Eagle's

medium supplemented with 10% FBS, 50 international units penicillin/streptomycin, and 2 mmol/liter L-glutamine (Invitrogen).

Western blotting

Cell or tissue lysates were prepared in radioimmune precipitation assay buffer (50 mM Tris-HCl (pH 8.0), 150 mM NaCl, 0.1% SDS, and 0.5% sodium deoxycholate, and 1% Nonidet P-40) with fresh proteinase inhibitor. An equal amount of protein was loaded. Western blot detection was carried out using a Li-Cor Odyssey image reader by software Image Studio (ver. 2.1). Antibodies used were as follows: phospho-Stat5 (Tyr-694) (C71E5, Cell Signaling Technology, dilution 1:1000), Stat5 (89, BD Biosciences, dilution 1:250), CAV1 (2297, BD Biosciences, dilution 1:1000), E2F1 (KH95, dilution 1:1000, Santa Cruz Biotechnology), E2F2 (TFE-25, dilution 1:1000, Santa Cruz Biotechnology), E2F3 (C-18, dilution 1:1000, Santa Cruz Biotechnology), and Rb (IF8, dilution 1:1000, Santa Cruz Biotechnology), β-actin (AC-15, Santa Cruz Biotechnology, dilution 1:3000), and goat anti-mouse/rabbit IRDye (Li-Cor, dilution 1:10000). The band intensity was measured by Image Studio (ver.2.1). The quantified data were calculated from three independent experiments.

ChIP

Cells were cross-linked by 0.75% formaldehyde in culture medium with gentle shaking for 10 min at room temperature and neutralized with a final concentration of 0.125 M glycine. After two washes with cold 1× PBS, cells were harvested in cold ChIP lysis buffer (50 mM HEPES-KOH (pH 7.5), 140 mM NaCl, 1 mM EDTA (pH 8.0), 1% Triton X-100, 0.1% sodium deoxycholate, 0.1% SDS, and fresh proteinase inhibitors), and sonicated to about 500 bp. The supernatants were used for immunoprecipitation by E2F3 antibody (C-18, Santa Cruz Biotechnology). After intensive washes, the proteins were eluted by elution buffer (0.1 M $NaHCO_3$ and 1% SDS). After reverse cross-linking, the DNA samples were recovered by phenol extraction and ethanol precipitation. The purified DNA was analyzed by quantitative PCR as described previously (52). The primers used were as follows: CAV1 ChIP forward, 5′-ACGCCTCTCGGTGGTTCAG-3′; CAV1 ChIP reverse, 5′-AAGGTTCTGGCAGCAGAGG-3′; CAV1 ChIP control forward, 5′-CTAACAAGCTCCCTGGATGC-3′; CAV1 ChIP control reverse, 5′-GTTTCTTCTCTTGTCTGTCTGTAGC-3′; mouse CAV1 ChIP forward, 5′-ATGCCTCTCTGTAGGTTTATAGC-3′; mouse CAV1 ChIP reverse, the same as CAV1 ChIP reverse; mouse CAV1 ChIP control forward, 5′-AGTCACGACTCTACCATGTGAAG-3′; mouse CAV1 ChIP control reverse, 5′-AGGTGAGGAGTCATGGAGTTCTC-3′.

Lentivirus production and CRISPR/Cas9

Human E2F3 cDNA was subcloned into the lentiviral expression vector pCDH-CMV-EF1-puro (System Biosciences). The lentiCRISPRv2 expression system was used to construct lentiviral CRISPR for CAV1 and E2F3 as described previously (53). The sequences of CAV1 CRISPR were as follows: CAV1 Oligo1, 5′-CACCGGGGCAAATACGTAGACTCCG-3′; CAV1 Oligo2, 5′-AAACCGGAGTCTACGTATTTGCCCC-3′. The sequences of E2F3 CRISPR were as follows: E2F3 Oligo1, 5′-CACCGACGCGGTATGATACGTCCCT-3′; E2F3 Oligo2, 5′-AAACAGGGACGTATCATACCGCGTC-3′. Production of lentivirus was performed as described previously (54). A single clone was established after puromycin selection. The genomic DNA of each clone was extracted for PCR to detect the indel mutation in the targeted region. Primers used were as follows: CAV1 detection forward, 5′-TGATGAAGGCTTTCTCACAGGC-3′; CAV1 detection reverse, 5′-ACTTTTCTAAGTCTGGCAGACCG-3′; E2F3 detection forward, 5′-AAAATGCCATTGCCAACATAGG-3′; E2F3 detection reverse, 5′-AGAGAGTGGGCTCCTACTCAC-3′. The PCR products were verified by sequencing.

RNA isolation and quantitative real-time PCR

Total RNA was isolated from cells or mouse tissue using TRIzol (Invitrogen) for RT-PCR. Total RNA (2 μg) was reverse-transcribed using Moloney murine leukemia virus reverse transcriptase (Promega) and random primers following the protocol of the manufacturer. PCR was performed in triplicate using SYBR Green Mix (Biotool) and a real-time PCR system (Bio-Rad) under the following conditions: 3 min at 95 °C followed by 45 cycles of 95 °C for 20 s 60 °C for 30 s and 65 °C for 1 min. Primers used were as follows: CCNE1 forward, 5′-GGAAGACTCCCACAACATCC-3′; CCNE1 reverse, 5′-GTCTCCTGCTCGCTGCTCTG-3′; CCNA2 forward, 5′-GCTTCAGCTTGTAGGCACGG-3′; CCNA2 reverse, 5′-ACTGTTGGTGCAGCCAAGTC-3′; PCNA forward, 5′-CTGCAAGTGGAGAGCTTGGC-3′; PCNA reverse, 5′-GTAGGAGACAGTGGAGTGGC-3′; CCND1 forward, 5′-TTCCTCTCCAAAATGCCAGA-3′; CCND1 reverse, 5′-AGGGTGGGTTGGAAATGAAC-3′; WAP forward, 5′-TCATCAGCCTTGTTCTTGGC-3′; WAP reverse, 5′-GCTTTTGGGAACATGGACTG-3′; CSN2 forward, 5′-TCGACTTTGCTGAAGTGTGG-3′; CSN2 reverse, 5′-TGACTGGATGCTGGAGTGAA-3′; GJB2 forward, 5′-TTCAGACCTGCTCCTTACCG-3′; GJB2 reverse, 5′-TTGTCCTCTGGATGGTTGGC-3′; JAK2 forward, 5′-GGCGGTGTTAGACATGATGAG-3′; JAK2 reverse, 5′-GCTCGAACGCACTTTGGTAA-3′; ERBB4 forward, 5′-CTCAATGAAACAACTGGCCC-3′; ERBB4 reverse, 5′-ACACACTCCCAATAGGCGAA-3′; PRLR forward, 5′-GGGGCCAAAAATAAAAGGATT-3′; PRLR reverse, 5′-TTGGAAAAAGACATGGCAGAA-3′; ELF5 forward, 5′-GACGCAGGAGGAGTTCATTG-3′; ELF5 reverse, 5′-CCAGTCTTGGTCTCTTCAGCA-3′; CAV1 forward, 5′-GCACACCAAGGAGATTGACC-3′; CAV1 reverse, 5′-AGATGCCGTCGAAACTGTGT-3′; SMAD3 forward, 5′-TAACTTCCCTGCTGGCATTG-3′; SMAD3 reverse, 5′-TCCATGCTGTGGTTCATCTG-3′; SOCS3 forward, 5′-AGATTTCGCTTCGGGACTAG-3′; SOCS3 reverse, 5′-AAACTTGCTGTGGGTGACC-3′; AQP5 forward, 5′-CCTGCGGTGGTCATGAAT-3′; AQP5 reverse, 5′-GTAGAGGATTGCAGCCAGGA-3′; NPT2B forward, 5′-ACTTGTTCGTGTGCTCCCTG-3′; NPT2B reverse, 5′-TGTTGCTGAAGAACTGTCCG-3′.

Whole-mount staining of mouse mammary glands

The entire no. 4 inguinal mammary gland was removed and spread onto a microscope slide. The tissue was fixed in Kahle's fix solution and stained in carmine alum solution using stan-

dard protocols. The stained mammary glands were imaged under a microscope. The images were analyzed with the MammoQuant software developed by Drs. Lee Hwee Kuan and Chow Yuan Ing to determine the number of the internal segments in each gland (31).

Histology

Mice were injected with bromodeoxyuridine and processed as described previously (55). Tissue samples were fixed in 10% buffered formalin and embedded in paraffin. Sections (6 μm) were stained with hematoxylin and eosin according to standard protocols. To calculate the relative alveolar area in the mammary glands, 10 randomly picked areas from H&E sections were analyzed for each genotype. The averages of the percentage of pixels occupied by alveoli were determined for each genotype using Adobe Photoshop similarly as described previously (56). For immunostaining, sections were dewaxed, rehydrated, and treated with 3% hydrogen peroxide to inhibit endogenous peroxidase activity. Antigen retrieval for all antibodies was performed by boiling in 10 mM sodium citrate (pH 6.0) for 10 min in a microwave (55). The slides were cooled down to room temperature and blocked in 10% natural goat serum in 1× Tris-buffered saline with 0.1% Tween 20 for 1 h. Slides were incubated overnight at 4 °C in primary antibody and then washed and incubated in secondary antibody for 1 h at room temperature. Slides were developed with 3,3′-diaminobenzidine (Amresco). After development, slides were lightly counterstained with hematoxylin. Antibodies used were as follows: phospho-Stat5 (Tyr-694) (C71E5, Cell Signaling Technology, dilution 1:400), Stat5 (89, BD Biosciences, dilution 1:100), CAV1 (2297, BD Biosciences, dilution 1:100), Ki67 (TEC-3, Dako Cytomation, dilution 1:25), bromodeoxyuridine (G3G4, Hybridoma Bank, dilution 1:10), and peroxidase-conjugated goat anti-mouse/rabbit IgG (Jackson ImmunoResearch Laboratories, dilution 1:200). The significant difference in Ki67 and pStat5 staining between mice was determined by counting 300–500 epithelial nuclei from 3–5 random tissue sections per mouse.

Statistics

The p values were determined using Student's unpaired t test.

Author contributions—Y. L. data curation; Y. L. formal analysis; Y. L. investigation; Y. L. and W. D. methodology; Y. L. and W. D. writing-original draft; Y. L. and W. D. project administration; Y. L. and W. D. writing-review and editing; W. D. conceptualization; W. D. supervision; W. D. funding acquisition.

Acknowledgments—We thank the mouse transgenic facility at the University of Chicago for generating the knockin mouse, Drs. Lee Hwee Kuan and Chow Yuan Ing for help with analysis using MammoQuant, and Dr. Zhe Li for the HC11 cells. We thank the Developmental Studies Hybridoma Bank (created by NICHD, National Institutes of Health and maintained at the University of Iowa) for providing some antibodies. We also thank the members of the Du laboratory for many discussions.

References

1. Trimarchi, J. M., and Lees, J. A. (2002) Sibling rivalry in the E2F family. *Nat. Rev. Mol. Cell Biol.* **3,** 11–20 CrossRef Medline
2. Chen, H. Z., Tsai, S. Y., and Leone, G. (2009) Emerging roles of E2Fs in cancer: an exit from cell cycle control. *Nat. Rev. Cancer* **9,** 785–797 CrossRef Medline
3. Gordon, G. M., and Du, W. (2011) Conserved RB functions in development and tumor suppression. *Protein Cell* **2,** 864–878 CrossRef Medline
4. van den Heuvel, S., and Dyson, N. J. (2008) Conserved functions of the pRB and E2F families. *Nat. Rev. Mol. Cell Biol.* **9,** 713–724 CrossRef Medline
5. Ren, B., Cam, H., Takahashi, Y., Volkert, T., Terragni, J., Young, R. A., and Dynlacht, B. D. (2002) E2F integrates cell cycle progression with DNA repair, replication, and G_2/M checkpoints. *Genes Dev.* **16,** 245–256 CrossRef Medline
6. Dimova, D. K., Stevaux, O., Frolov, M. V., and Dyson, N. J. (2003) Cell cycle-dependent and cell cycle-independent control of transcription by the *Drosophila* E2F/RB pathway. *Genes Dev.* **17,** 2308–2320 CrossRef Medline
7. Du, W. (2000) Suppression of the rbf null mutants by a de2f1 allele that lacks transactivation domain. *Development* **127,** 367–379 Medline
8. Tsai, K. Y., Hu, Y., Macleod, K. F., Crowley, D., Yamasaki, L., and Jacks, T. (1998) Mutation of E2f-1 suppresses apoptosis and inappropriate S phase entry and extends survival of Rb-deficient mouse embryos. *Mol. Cell* **2,** 293–304 CrossRef Medline
9. Yamasaki, L., Bronson, R., Williams, B. O., Dyson, N. J., Harlow, E., and Jacks, T. (1998) Loss of E2F-1 reduces tumorigenesis and extends the lifespan of Rb1(+/−)mice. *Nat. Genet.* **18,** 360–364 CrossRef Medline
10. Ziebold, U., Reza, T., Caron, A., and Lees, J. A. (2001) E2F3 contributes both to the inappropriate proliferation and to the apoptosis arising in Rb mutant embryos. *Genes Dev.* **15,** 386–391 CrossRef Medline
11. Ziebold, U., Lee, E. Y., Bronson, R. T., and Lees, J. A. (2003) E2F3 loss has opposing effects on different pRB-deficient tumors, resulting in suppression of pituitary tumors but metastasis of medullary thyroid carcinomas. *Mol. Cell. Biol.* **23,** 6542–6552 CrossRef Medline
12. Kratzke, R. A., Otterson, G. A., Hogg, A., Coxon, A. B., Geradts, J., Cowell, J. K., and Kaye, F. J. (1994) Partial inactivation of the RB product in a family with incomplete penetrance of familial retinoblastoma and benign retinal tumors. *Oncogene* **9,** 1321–1326 Medline
13. Otterson, G. A., Chen, Wd., Coxon, A. B., Khleif, S. N., and Kaye, F. J. (1997) Incomplete penetrance of familial retinoblastoma linked to germline mutations that result in partial loss of RB function. *Proc. Natl. Acad. Sci. U.S.A.* **94,** 12036–12040 CrossRef Medline
14. Sun, H., Wang, Y., Chinnam, M., Zhang, X., Hayward, S. W., Foster, B. A., Nikitin, A. Y., Wills, M., and Goodrich, D. W. (2011) E2f binding-deficient Rb1 protein suppresses prostate tumor progression *in vivo*. *Proc. Natl. Acad. Sci. U.S.A.* **108,** 704–709 CrossRef Medline
15. Cecchini, M. J., Thwaites, M. J., Talluri, S., MacDonald, J. I., Passos, D. T., Chong, J. L., Cantalupo, P., Stafford, P. M., Sáenz-Robles, M. T., Francis, S. M., Pipas, J. M., Leone, G., Welch, I., and Dick, F. A. (2014) A retinoblastoma allele that is mutated at its common E2F interaction site inhibits cell proliferation in gene-targeted mice. *Mol. Cell. Biol.* **34,** 2029–2045 CrossRef Medline
16. Lee, E. Y., Cam, H., Ziebold, U., Rayman, J. B., Lees, J. A., and Dynlacht, B. D. (2002) E2F4 loss suppresses tumorigenesis in Rb mutant mice. *Cancer Cell* **2,** 463–472 CrossRef Medline
17. Weng, L., Zhu, C., Xu, J., and Du, W. (2003) Critical role of active repression by E2F and Rb proteins in endoreplication during *Drosophila* development. *EMBO J.* **22,** 3865–3875 CrossRef Medline
18. Liao, Y., and Du, W. (2017) Rb-independent E2F3 promotes cell proliferation and alters expression of genes involved in metabolism and inflammation. *FEBS Open Bio* **7,** 1611–1621 CrossRef Medline
19. Visvader, J. E. (2009) Keeping abreast of the mammary epithelial hierarchy and breast tumorigenesis. *Genes Dev.* **23,** 2563–2577 CrossRef Medline

20. Watson, C. J., and Khaled, W. T. (2008) Mammary development in the embryo and adult: a journey of morphogenesis and commitment. *Development* **135,** 995–1003 CrossRef Medline
21. Hennighausen, L., and Robinson, G. W. (2005) Information networks in the mammary gland. *Nat. Rev. Mol. Cell Biol.* **6,** 715–725 CrossRef Medline
22. Gallego, M. I., Binart, N., Robinson, G. W., Okagaki, R., Coschigano, K. T., Perry, J., Kopchick, J. J., Oka, T., Kelly, P. A., and Hennighausen, L. (2001) Prolactin, growth hormone, and epidermal growth factor activate Stat5 in different compartments of mammary tissue and exert different and overlapping developmental effects. *Dev. Biol.* **229,** 163–175 CrossRef Medline
23. Brisken, C., and O'Malley, B. (2010) Hormone action in the mammary gland. *Cold Spring Harb. Perspect. Biol.* **2,** a003178 Medline
24. Teglund, S., McKay, C., Schuetz, E., van Deursen, J. M., Stravopodis, D., Wang, D., Brown, M., Bodner, S., Grosveld, G., and Ihle, J. N. (1998) Stat5a and Stat5b proteins have essential and nonessential, or redundant, roles in cytokine responses. *Cell* **93,** 841–850 CrossRef Medline
25. Liu, X., Robinson, G. W., Wagner, K. U., Garrett, L., Wynshaw-Boris, A., and Hennighausen, L. (1997) Stat5a is mandatory for adult mammary gland development and lactogenesis. *Gene Dev* **11,** 179–186 CrossRef Medline
26. Miyoshi, K., Shillingford, J. M., Smith, G. H., Grimm, S. L., Wagner, K. U., Oka, T., Rosen, J. M., Robinson, G. W., and Hennighausen, L. (2001) Signal transducer and activator of transcription (Stat) 5 controls the proliferation and differentiation of mammary alveolar epithelium. *J. Cell Biol.* **155,** 531–542 CrossRef Medline
27. Park, D. S., Lee, H., Frank, P. G., Razani, B., Nguyen, A. V., Parlow, A. F., Russell, R. G., Hulit, J., Pestell, R. G., and Lisanti, M. P. (2002) Caveolin-1-deficient mice show accelerated mammary gland development during pregnancy, premature lactation, and hyperactivation of the Jak-2/STAT5a signaling cascade. *Mol. Biol. Cell* **13,** 3416–3430 CrossRef
28. Tonko-Geymayer, S., Goupille, O., Tonko, M., Soratroi, C., Yoshimura, A., Streuli, C., Ziemiecki, A., Kofler, R., and Doppler, W. (2002) Regulation and function of the cytokine-inducible SH-2 domain proteins, CIS and SOCS3, in mammary epithelial cells. *Mol. Endocrinol.* **16,** 1680–1695 CrossRef Medline
29. Cocolakis, E., Dai, M., Drevet, L., Ho, J., Haines, E., Ali, S., and Lebrun, J. J. (2008) Smad signaling antagonizes STAT5-mediated gene transcription and mammary epithelial cell differentiation. *J. Biol. Chem.* **283,** 1293–1307 CrossRef Medline
30. Park, D. S., Lee, H., Riedel, C., Hulit, J., Scherer, P. E., Pestell, R. G., and Lisanti, M. P. (2001) Prolactin negatively regulates caveolin-1 gene expression in the mammary gland during lactation, via a Ras-dependent mechanism. *J. Biol. Chem.* **276,** 48389–48397 CrossRef
31. Law, Y. N., Racine, V., Ang, P. L., Mohamed, H., Soo, P. C., Veltmaat, J. M., and Lee, H. K. (2012) Development of MammoQuant: an automated quantitative tool for standardized image analysis of murine mammary gland morphogenesis. *J. Med. Imaging Health Inform.* **2,** 352–365 CrossRef
32. Shillingford, J. M., Miyoshi, K., Robinson, G. W., Bierie, B., Cao, Y., Karin, M., and Hennighausen, L. (2003) Proteotyping of mammary tissue from transgenic and gene knockout mice with immunohistochemical markers: a tool to define developmental lesions. *J. Histochem. Cytochem.* **51,** 555–565 CrossRef Medline
33. Brisken, C., Kaur, S., Chavarria, T. E., Binart, N., Sutherland, R. L., Weinberg, R. A., Kelly, P. A., and Ormandy, C. J. (1999) Prolactin controls mammary gland development via direct and indirect mechanisms. *Dev. Biol.* **210,** 96–106 CrossRef Medline
34. Fata, J. E., Kong, Y. Y., Li, J., Sasaki, T., Irie-Sasaki, J., Moorehead, R. A., Elliott, R., Scully, S., Voura, E. B., Lacey, D. L., Boyle, W. J., Khokha, R., and Penninger, J. M. (2000) The osteoclast differentiation factor osteoprotegerin-ligand is essential for mammary gland development. *Cell* **103,** 41–50 CrossRef Medline
35. Bist, A., Fielding, C. J., and Fielding, P. E. (2000) p53 regulates caveolin gene transcription, cell cholesterol, and growth by a novel mechanism. *Biochemistry* **39,** 1966–1972 CrossRef
36. Ball, R. K., Friis, R. R., Schoenenberger, C. A., Doppler, W., and Groner, B. (1988) Prolactin regulation of beta-casein gene-expression and of a cytosolic 120-kd protein in a cloned mouse mammary epithelial-cell line. *EMBO J.* **7,** 2089–2095 Medline
37. Shalem, O., Sanjana, N. E., Hartenian, E., Shi, X., Scott, D. A., Mikkelson, T. S., Heckl, D., Ebert, B. L., Root, D. E., Doench, J. G., and Zhang, F. (2014) Genome-scale CRISPR-Cas9 knockout screening in human cells. *Science* **343,** 84–87 CrossRef Medline
38. Williams, T. M., Medina, F., Badano, I., Hazan, R. B., Hutchinson, J., Muller, W. J., Chopra, N. G., Scherer, P. E., Pestell, R. G., and Lisanti, M. P. (2004) Caveolin-1 gene disruption promotes mammary tumorigenesis and dramatically enhances lung metastasis *in vivo*: role of Cav-1 in cell invasiveness and matrix metalloproteinase (MMP-2/9) secretion. *J. Biol. Chem.* **279,** 51630–51646 CrossRef Medline
39. Williams, T. M., Cheung, M. W., Park, D. S., Razani, B., Cohen, A. W., Muller, W. J., Di Vizio, D., Chopra, N. G., Pestell, R. G., and Lisanti, M. P. (2003) Loss of caveolin-1 gene expression accelerates the development of dysplastic mammary lesions in tumor-prone transgenic mice. *Mol. Biol. Cell* **14,** 1027–1042 CrossRef Medline
40. Williams, T. M., Sotgia, F., Lee, H., Hassan, G., Di Vizio, D., Bonuccelli, G., Capozza, F., Mercier, I., Rui, H., Pestell, R. G., and Lisanti, M. P. (2006) Stromal and epithelial caveolin-1 both confer a protective effect against mammary hyperplasia and tumorigenesis: Caveolin-1 antagonizes cyclin D1 function in mammary epithelial cells. *Am. J. Pathol.* **169,** 1784–1801 CrossRef Medline
41. Sloan, E. K., Ciocca, D. R., Pouliot, N., Natoli, A., Restall, C., Henderson, M. A., Fanelli, M. A., Cuello-Carrión, F. D., Gago, F. E., and Anderson, R. L. (2009) Stromal cell expression of caveolin-1 predicts outcome in breast cancer. *Am. J. Pathol.* **174,** 2035–2043 CrossRef Medline
42. Jiang, Z., Deng, T., Jones, R., Li, H., Herschkowitz, J. I., Liu, J. C., Weigman, V. J., Tsao, M. S., Lane, T. F., Perou, C. M., and Zacksenhaus, E. (2010) Rb deletion in mouse mammary progenitors induces luminal-B or basal-like/EMT tumor subtypes depending on p53 status. *J. Clin. Invest.* **120,** 3296–3309 CrossRef Medline
43. Francis, S. M., Bergsied, J., Isaac, C. E., Coschi, C. H., Martens, A. L., Hojilla, C. V., Chakrabarti, S., Dimattia, G. E., Khoka, R., Wang, J. Y., and Dick, F. A. (2009) A functional connection between pRB and transforming growth factor β in growth inhibition and mammary gland development. *Mol. Cell. Biol.* **29,** 4455–4466 CrossRef Medline
44. Shan, B., Chang, C. Y., Jones, D., and Lee, W. H. (1994) The transcription factor E2F-1 mediates the autoregulation of RB gene expression. *Mol. Cell. Biol.* **14,** 299–309 CrossRef Medline
45. Herrera, R. E., Sah, V. P., Williams, B. O., Mäkelä, T. P., Weinberg, R. A., and Jacks, T. (1996) Altered cell cycle kinetics, gene expression, and G_1 restriction point regulation in Rb-deficient fibroblasts. *Mol. Cell. Biol.* **16,** 2402–2407 CrossRef Medline
46. Humbert, P. O., Verona, R., Trimarchi, J. M., Rogers, C., Dandapani, S., and Lees, J. A. (2000) E2f3 is critical for normal cellular proliferation. *Genes Dev.* **14,** 690–703 Medline
47. Feber, A., Clark, J., Goodwin, G., Dodson, A. R., Smith, P. H., Fletcher, A., Edwards, S., Flohr, P., Falconer, A., Roe, T., Kovacs, G., Dennis, N., Fisher, C., Wooster, R., Huddart, R., *et al.* (2004) Amplification and overexpression of E2F3 in human bladder cancer. *Oncogene* **23,** 1627–1630 CrossRef Medline
48. Foster, C. S., Falconer, A., Dodson, A. R., Norman, A. R., Dennis, N., Fletcher, A., Southgate, C., Dowe, A., Dearnaley, D., Jhavar, S., Eeles, R., Feber, A., and Cooper, C. S. (2004) Transcription factor E2F3 overexpressed in prostate cancer independently predicts clinical outcome. *Oncogene* **23,** 5871–5879 CrossRef Medline
49. Lawrence, M. S., Stojanov, P., Mermel, C. H., Robinson, J. T., Garraway, L. A., Golub, T. R., Meyerson, M., Gabriel, S. B., Lander, E. S., and Getz, G. (2014) Discovery and saturation analysis of cancer genes across 21 tumour types. *Nature* **505,** 495–501 CrossRef Medline
50. Forbes, S. A., Beare, D., Gunasekaran, P., Leung, K., Bindal, N., Boutselakis, H., Ding, M., Bamford, S., Cole, C., Ward, S., Kok, C. Y., Jia, M., De, T., Teague, J. W., Stratton, M. R., *et al.* (2015) COSMIC: exploring the world's knowledge of somatic mutations in human cancer. *Nucleic Acids Res.* **43,** D805-D811 CrossRef Medline

51. Forster, N., Saladi, S. V., van Bragt, M., Sfondouris, M. E., Jones, F. E., Li, Z., and Ellisen, L. W. (2014) Basal cell signaling by p63 controls luminal progenitor function and lactation via NRG1. *Dev. Cell* **28,** 147–160 CrossRef Medline
52. Zhang, T., and Du, W. (2015) Groucho restricts rhomboid expression and couples EGFR activation with R8 selection during *Drosophila* photoreceptor differentiation. *Dev. Biol.* **407,** 246–255 CrossRef Medline
53. Sanjana, N. E., Shalem, O., and Zhang, F. (2014) Improved vectors and genome-wide libraries for CRISPR screening. *Nat. Methods* **11,** 783–784 CrossRef Medline
54. Li, B., Gordon, G. M., Du, C. H., Xu, J., and Du, W. (2010) Specific killing of Rb mutant cancer cells by inactivating TSC2. *Cancer Cell* **17,** 469–480 CrossRef Medline
55. Pogoriler, J., Millen, K., Utset, M., and Du, W. (2006) Loss of cyclin D1 impairs cerebellar development and suppresses medulloblastoma formation. *Development* **133,** 3929–3937 CrossRef Medline
56. Gordon, G. M., Zhang, T., Zhao, J., and Du, W. (2013) Deregulated G_1-S control and energy stress contribute to the synthetic-lethal interactions between inactivation of RB and TSC1 or TSC2. *J. Cell Sci.* **126,** 2004–2013 CrossRef Medline